

Ectopic Expression of Cell Cycle Markers in Models of Induced Programmed Cell Death in Dopamine Neurons of the Rat Substantia Nigra Pars Compacta

Bassem F. El-Khodor,* Tinmarla Frances Oo,* Nikolai Kholodilov,* and Robert E. Burke*†¹

*Department of Neurology and †Department of Pathology, The College of Physicians and Surgeons, Columbia University, New York, New York 10032

Received October 3, 2001; accepted August 21, 2002

There is increasing evidence that proteins normally involved in the cell cycle can regulate neuronal programmed cell death (PCD). However, it remains unknown whether cell cycle markers are expressed in normal, postmitotic, postmigratory neurons undergoing PCD *in vivo*. We have previously shown that natural cell death occurs postnatally in dopamine neurons of the substantia nigra pars compacta (SNpc). PCD can be induced postnatally in these neurons either by intrastriatal injection of the neurotoxin 6-hydroxydopamine (6-OHDA) or by medial forebrain bundle (MFB) axotomy. At the time of induction of death in these models, these neurons are long postmitotic and postmigratory. We have studied three cell cycle markers in these models: 5-bromo-2'-deoxyuridine (BrdU) incorporation (a marker of S phase), cdc2 protein expression (a marker of G2 phase), and expression of MPM2 (a marker of M phase), an epitope phosphorylated by cdc2. We report here that postmitotic dopaminergic neurons undergoing PCD in the SNpc following 6-OHDA and axotomy lesions incorporate BrdU and overexpress cdc2, but do not express MPM2. This is the first *in vivo* evidence that postmitotic dopamine neurons of the SNpc undergoing apoptosis express markers for S phase and G2 phase. These results raise the possibility that cell cycle regulatory proteins may play a role in the demise of dopaminergic neurons in Parkinson's disease, in which PCD has been postulated to play a role. © 2002 Elsevier Science (USA)

Key Words: postmitotic neuron; dopamine; apoptosis; MPM2; Cdc2; 5-bromo-2'-deoxyuridine; axotomy; medial forebrain bundle; 6-OHDA; Parkinson's disease.

INTRODUCTION

There is growing evidence that regulators of the cell cycle may be important mediators of programmed cell death (PCD) (for reviews, see Lundberg and Weinberg (28) and O'Connor *et al.* (36)). Early observations in nonneural systems demonstrated that the c-myc oncogene plays a direct role in mediating PCD (2, 9, 46). In neural systems, in tissue culture, early investigations also implicated cell cycle regulation in PCD (11, 12), and many subsequent observations have particularly implicated the cyclin-dependent kinases (cdks), the retinoblastoma protein (pRb), and related proteins. Cyclin D1, which activates cdks early in the G1 phase, is upregulated in sympathetic neurons induced to die by nerve growth factor (NGF) withdrawal (12), and expression of the cyclin D-dependent kinase inhibitor p16^{INK4A} protects neurons from apoptotic death (25). Pharmacologic inhibitors of the cdks suppress PCD of PC12 cells and sympathetic neurons following withdrawal of trophic support (39) and death in PC12 cells induced by DNA-damaging agents (42). Genetic approaches, utilizing either expression of dominant negative forms of cdks, or expression of cdk inhibitors, have likewise suppressed PCD induced by trophic factor withdrawal (40) or DNA damage (43). These studies have specifically implicated cdk4 and -6, but not cdk2 or -3, in PCD. Cdks 4/6 phosphorylate the pRb family members, which regulate the transcriptional activity of E2F/DP1 complexes. Neuron death induced by DNA damage is associated with phosphorylation of pRb, and it is suppressed by expression of a dominant negative form of DP1 (41), as is death induced by β -amyloid toxicity (14).

These *in vitro* studies in neural cells are supported by observations *in vivo*. Overexpression of the pRb-binding protein SV40 T antigen in postmitotic Purkinje cells in transgenic mice results in the induction of apoptotic death, which is accompanied by 5-bromo-2'-

¹ To whom correspondence should be addressed at Department of Neurology, Room 308, Black Building, Columbia University, 650 West 168th Street, New York, NY 10032. Fax: (212) 305-5450. E-mail: rb43@columbia.edu.

deoxyuridine (BrdU) incorporation in the nuclear DNA of the dying cells (10). Similarly, overexpression of SV40 T antigen in retinal neurons results in their death (16). In the setting of augmented natural cell death in mouse mutants with developmental defects of the cerebellum, three cell cycle markers are expressed in dying granule cells: cyclin D, proliferating cell nuclear antigen (PCNA), and BrdU incorporation (20). In the course of normal development in the cortex, apoptosis is observed in the proliferative zone, and many of the dying cells incorporate BrdU (48).

These observations of a close relationship between PCD and cell cycle regulation may have important implications for the pathogenesis of human disease. Immunostaining of MPM2, a marker for mitotic phosphoepitopes, has been identified in neurofibrillary tangle-bearing neurons in Alzheimer's disease (51). M-phase phosphoepitopes are generated by *cdc2*/cyclin B1 kinase, and these proteins are also expressed in neurons with neurofibrillary tangles in Alzheimer brains (50). Others have confirmed overexpression of cyclin B1 and have identified overexpression of cyclin D, *cdk4*, and PCNA (1). The functional significance of the expression of these regulators of the cell cycle is suggested by the recent observation of DNA replication within neurons of the Alzheimer brain (53). The general significance of these observations in Alzheimer's disease is supported by the demonstration of mitotic indices in a variety of neurodegenerative disorders including progressive supranuclear palsy, cortico-basal-ganglionic degeneration, and others (21).

These findings indicate that it is important to understand the precise relationship between cell cycle regulation and PCD in living brain. There is especially a need to understand whether cell cycle markers are expressed in conjunction with PCD in normal, postmitotic, postmigratory neurons. As summarized above, most of the observations made to date *in vivo* have been made in transgenic or mutant murine models, or, in one study in normal rats, in periventricular zones where there is ongoing cellular proliferation (48) and subsequent migration. In addition, there is a need to study these events in phenotypically identified neurons which are known to be involved in human neurodegenerative disease. We have shown that natural cell death occurs in dopamine neurons of the substantia nigra (SN) (22, 37), the neurons which degenerate in Parkinson's disease. This event can be induced postnatally either by intrastriatal injection of the neurotoxin 6-hydroxydopamine (6-OHDA) (31) or by medial forebrain bundle (MFB) axotomy (6). At the time of induction of death in these models, these neurons are long postmitotic (7, 27, 30) and postmigratory (47). We have therefore studied three cell cycle markers in these models: BrdU incorporation (a marker of S phase), *cdc2* protein expression (a marker of G2 phase), and expression of

MPM2 (a marker of M phase). We report here that postmitotic dopaminergic neurons undergoing apoptosis in the SNpc following 6-OHDA and axotomy lesions incorporate BrdU and overexpress *cdc2*, but do not express MPM2. This is the first *in vivo* demonstration that neuronal apoptosis in dopamine neurons of the SNpc involves abnormal expression of cell cycle markers.

MATERIALS AND METHODS

Animal Models

Timed pregnant Sprague-Dawley rats (14–16 days pregnant) were obtained from Charles River Laboratories (Wilmington, MA). The cage was inspected in the afternoon of each day, and the day of birth was defined as postnatal day (PND) 1. The MFB axotomy and 6-OHDA lesions were performed at PND 7 and rats were sacrificed at postlesion days (PLD) 2 and 7, respectively. The dates of sacrifice were based on our previous demonstration that induction of PCD in the SNpc peaks at PLD 2 following medial forebrain bundle transection (6) and at PLD 7 in the 6-OHDA model (31). All animal procedures have been approved by the Animal Care and Use Committee at Columbia-Presbyterian Medical Center.

Medial Forebrain Bundle Axotomy

The PND 7 rat pups were anesthetized by hypothermia. Animals were then positioned in a stereotaxic apparatus (Kopf Instruments, Tujunga, CA) to conform with the neonatal brain atlas described by Heller *et al.* (19). The apparatus is equipped with a hypothermic miniaturized stereotaxic adapter for neonatal rats (Stoelting Co., Wood Dale, IL). The MFB is transected as follows: a retractable wire knife (Kopf Instruments) is lowered through a hole 1.4 mm posterior and 2.5 mm lateral to the left of bregma to a ventral position of 6.5 mm below bregma. The blade is extended by 2 mm, and the knife is slowly moved upward by 2.5 mm, down by the same distance, up again, and finally down by 2.5 mm. The blade is then retracted and slowly removed from the brain. After recovery from anesthesia (approximately 2–3 h at 34°C), pups were returned to the dams until PLD 2.

6-OHDA Lesions

6-OHDA lesions were performed as previously described (31). Rat pups at PND 7 were pretreated with 25 mg/kg desmethylimipramine, anesthetized by hypothermia, and placed prone on an ice pack. The skull was exposed by a midline incision, and a burr hole was placed 3.0 mm lateral to the left of bregma on the coronal suture. A 28-gauge cannula was then inserted

vertically into the striatum to a depth of 4.0 mm from the top of the skull. 6-OHDA hydrobromide (Regis, Morton Grove, IL) was prepared at 15 μg (total weight)/1.0 μl in 0.9% NaCl/0.02% ascorbic acid, and infused by pump (Harvard Apparatus, Holliston, MA) at a rate of 0.25 $\mu\text{l}/\text{min}$. The cannula was slowly withdrawn 2 min after the end of the infusion. After recovery from anesthesia, pups were returned to the dams until PLD 7.

Brain Preparation and Immunohistochemistry

Brain Preparation

Rats at either PND 9 (2 days after MFB transection) or PND 14 (7 days after 6-OHDA lesion) were anesthetized with halothane vapor and perfused with ice-cold 0.9% NaCl by gravity for 5 min. They were then perfused with ice-cold 4% paraformaldehyde/0.1 M phosphate buffer (PB) by gravity for 10 min. The brain was then carefully removed from the skull and postfixed in the same fixative for varying lengths of time at 4°C, depending on the primary antibody used. The brain was then cryoprotected in 20% w/w sucrose in 0.1 M PB for 48 h. The brains were then rapidly frozen in 2-methylbutane chilled on dry ice and sectioned on a cryostat through the entire SN at either 20 μm for cdc2 and MPM2 or 30 μm for BrdU/tyrosine hydroxylase (TH) immunofluorescence double labeling. For all protocols, sections were collected into wells containing phosphate-buffered saline (PBS) (pH 7.1) and processed free-floating. In each experiment, sections from axotomized and 6-OHDA-lesioned animals were run in parallel to allow a more accurate comparison of the level of expression of each protein between the two models.

Immunohistochemistry

For cdc2 staining, brains were postfixed for 24 h at 4°C. After washes in PBS, sections were treated in 0.1 M PBS/0.5 % bovine serum albumin (BSA) for 15 min at 4°C, followed by 30 min treatment in 0.1 M PBS/0.5 % BSA/ 0.1 % Triton at 4°C. Sections were then washed in PBS and incubated in primary antibody [Santa Cruz Biotechnology, Santa Cruz, CA; rabbit polyclonal anti-cdc2 (Cat. No. SC 954)] at 1:50 in PBS/BSA for 24 h at 4°C. Sections were washed in PBS/BSA and then incubated with biotinylated protein A, prepared in our laboratory, at 1:100 in PBS/BSA for 1 h at room temperature (RT). Sections were then washed with PBS/BSA and incubated with avidin-biotin-horseradish peroxidase complexes (ABC, Vector Laboratories, Burlingame, CA) at 1:600 for 1 h at RT. Following washes in PBS, sections were incubated in a solution of diaminobenzidine (50 mg in 100 ml Tris buffer at pH 7.6) containing glucose oxidase, ammonium chloride, and

D(+)-glucose to generate H_2O_2 . Following three 15-min washes in Tris buffer, pH 7.6, sections were then mounted on gelatin-coated slides, left to dry overnight at RT, and then Nissl-counterstained.

For MPM2 staining, brains were postfixed for 3 h at 4°C. After washes in PBS, sections were incubated in primary antibody [Upstate Biotechnology Inc., Lake Placid, NY; mouse monoclonal anti-MPM2 (Cat. No. 05-368)] at 1:200 in PBS/10% normal horse serum (NHS) for 24 h at 4°C. After a wash in PBS, sections were incubated in secondary antibody [Vector Laboratories; biotinylated horse anti-mouse IgG] at 1:50 in PBS/10% NHS for 24 h at 4°C. Sections were then processed as previously described for cdc2. After PBS wash, sections were incubated with avidin-biotinylated horseradish peroxidase complexes and then treated with diaminobenzidine in the presence of H_2O_2 . Sections were mounted on gelatin-coated slides and counterstained with Nissl.

For BrdU/TH immunofluorescence double labeling, brains were postfixed for 1 week at 4°C. Sections were washed in PBS twice for 15 min and then treated in 2.0 N HCl for 30 min at RT to expose BrdU epitopes. To neutralize the acid, sections were rinsed twice for 10 min with 0.1 M borate buffer, pH 8.5, at RT followed by two 15-min washes with PBS at 4°C. Sections were then treated for 15 min in PBS/10% NHS/10 % normal goat serum (NGS) at 4°C, followed by 30-min treatment in PBS/10% NHS/10% NGS/0.1% Triton at 4°C. After PBS wash, sections were incubated with either mouse monoclonal anti-BrdU at 1:400 (Cat. No. MAB 3424) (Chemicon International Inc, Temecula, CA) or rabbit polyclonal anti-TH at 1:1000 (Cat. No. 657012) (Calbiochem-Novabiochem Corporation, San Diego, CA) or both for 48 h at 4°C. Sections were then washed with Tris-buffered saline (TBS) and incubated with Texas red-conjugated horse anti-mouse at 1:75 (Vector Laboratories) and fluorescein-conjugated goat anti-rabbit at 1:75 (Vector Laboratories) in TBS/10% NHS/10% NGS/0.1% Triton for 1 h at RT. Following several washes in PBS, sections were mounted on gelatin-coated slides, left to dry overnight at RT, and then stained with Hoechst 33342 (Molecular Probes, Eugene, OR) at 1:500 to visualize apoptotic chromatin clumps. Sections were coverslipped with Dako anti-fade medium and viewed with appropriate filters by epifluorescence on a Nikon Eclipse 800 microscope. Images were captured with a Spot II digital camera and single channel images were merged using Adobe Photoshop. We have previously shown that BrdU labeling performed as we have described using a peroxidase technique specifically labels mitotic postnatal cerebellar granule cells (7).

In order to determine the cellular phenotypes from which apoptotic profiles were derived in the 6OHDA model we processed $n = 5$ rats in parallel for immu-

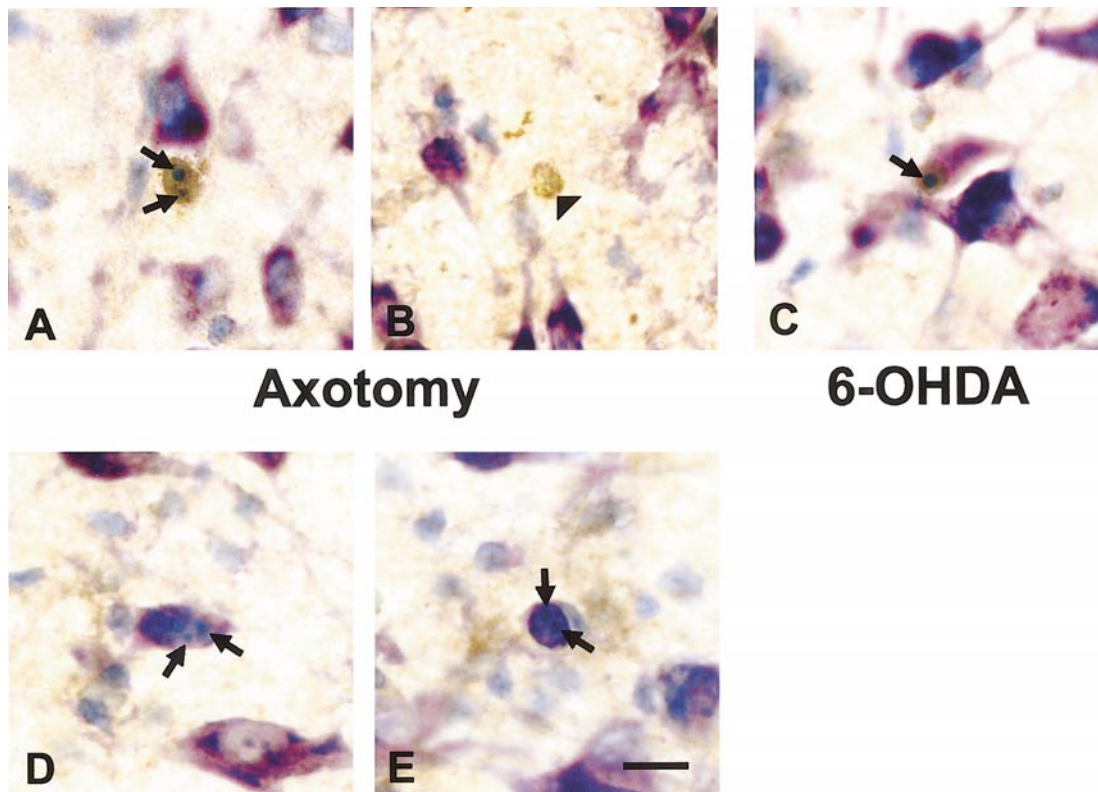


FIG. 1. Cdc2 immunoperoxidase stain and thionin counterstain of apoptotic profiles in SNpc following induction of cell death by axotomy (A and B) or 6-OHDA lesion (C). Arrows show round, basophilic, intranuclear chromatin clumps, characteristic of apoptosis. Axotomy was performed at PND 7 and animals were studied on PLD 2. Intrastratial 6-OHDA lesion was performed on PND 7 and animals were studied on PLD 7. Cdc2-positive apoptotic profiles were observed in late stages of cell death with an apparent loss of neuronal morphology and cytoplasm. Some cdc2-positive profiles showed either faint nuclear chromatin clumps or did not contain them at all (B) (black triangle). All early apoptotic profiles observed in the SNpc that retained neuronal morphology (D) or cytoplasm (E) were cdc2 negative. Bar = 10 μ m.

nohistochemistry for the neuronal marker NeuN (Chemicon, at 1:100), the astrocytic marker GFAP (DAKO, Carpinteria, CA, at 1:1000), and the microglial marker OX-42 (Serotec, Raleigh, NC, at 1:50) using secondary reagents as described, and diaminobenzidine as chromagen. After immunostaining, sections were thionin-counterstained to identify characteristic apoptotic chromatin clumps.

Qualitative and Quantitative Morphologic Analysis

Qualitative Morphologic Analysis

In the immunoperoxidase-stained material, apoptosis was identified at the light microscope level by performing a thionin counterstain and visualizing intranuclear chromatin clumps as one or more intensely basophilic, homogeneously stained, round, and distinctly bounded structures. We have previously shown for both the 6-OHDA and the axotomy models that apoptotic profiles so identified are confirmed to be apoptotic by suppressed silver staining, TUNEL labeling (6, 31), immunostaining for activated caspase-3 (6, 23) and its cleavage products (6, 38), and by electron mi-

croscopy (6, and unpublished observations). In the immunofluorescence double-labeled material, apoptotic profiles were identified by the presence of intensely fluorescent, round, and distinctly bounded structures within the nucleus on UV illumination of Hoechst 33342-stained sections.

Quantitative Morphologic Analysis

Apoptotic profiles in each SN were quantified by selecting 2 sections from each of Paxinos-Watson (44) SN planes 4.2, 3.7, and 3.2 and scanning the entire SN at 600 \times . Apoptotic profiles were identified as cellular profiles containing one or more distinct, rounded basophilic chromatin clumps. Free extracellular chromatin clumps, lying outside an identifiable cellular profile, were not counted. The number of profiles in the two sections in a given plane were averaged, to provide a measure for that plane, and then the averages for the three planes were added to provide an index of the number of profiles for each SN. We have previously shown, using a physical dissector technique (15), that apoptotic profiles, as defined, are rarely split by the

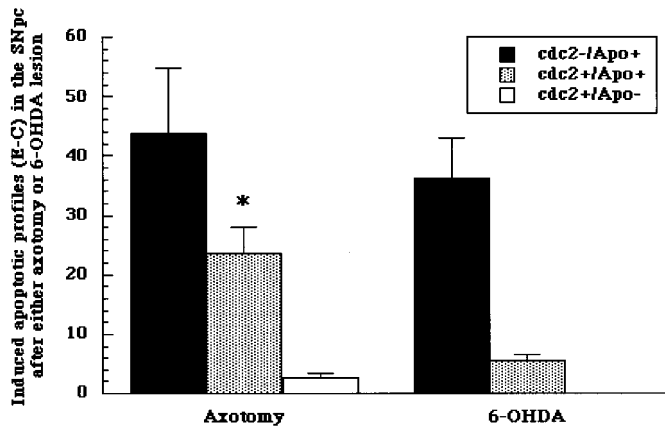


FIG. 2. Quantitative analysis of the induction of apoptotic profiles in the axotomy and 6-OHDA models. Three categories of profiles were quantified: cdc2-negative/ chromatin clump-positive (cdc2-/Apo+); cdc2-positive/ chromatin clump-positive (cdc2+/Apo+); and cdc2-positive/ chromatin clump-negative (cdc2+/Apo-). Since natural cell death occurs in SNpc during the same postnatal development period, the number of induced apoptotic profiles is expressed as the difference between the experimental (E) and control (C) sides. In both the 6OHDA model (31) and the axotomy model (6), the numbers of apoptotic profiles on the Control side were $\leq 10\%$ of their numbers on the Experimental side. An n of 4 was analyzed for each model of induced cell death for a total of 8 animals. Student's t test showed that the number of cdc2-positive apoptotic profiles in axotomy was significantly higher than the 6-OHDA model ($t = 3.88$; $*P = 0.0082$). There was no significant difference in the induction of cdc2-negative apoptotic profiles between axotomy and 6-OHDA lesions ($t = 0.58$; $P = 0.5805$). cdc2+/Apo- profiles were observed only in the axotomy model.

microtome blade (37). Clarke and Oppenheim have demonstrated a similar result (3). Thus apoptotic profiles, identified by focusing through the section, represent unique and unbiased counts. At least 50 apoptotic profiles/ brain ($n = 4$ animals/model) were assessed for immunoperoxidase labeling for MPM2.

Western Analysis

To confirm the monospecificity of the anti-cdc2 antibody, and to examine cdc2 protein expression at the tissue level, Western analysis was performed. Four PND7 rats underwent unilateral 6OHDA lesion and were sacrificed at PLD6. The SN on the lesioned and contralateral, nonlesioned sides were microdissected as previously described (34). Cerebellar tissue from a PND2 rat was included as a positive control for cdc2 protein. Tissue was homogenized in buffer containing final concentrations of Tris-HCl 50 mM, NaCl 150 mM, EDTA 2 mM, Nonidet P-40 1%, aprotinin 5 $\mu\text{g/ml}$, leupeptin 5 $\mu\text{g/ml}$, PMSF 17 $\mu\text{g/ml}$. Final protein concentration was determined, and 90 μg of each sample was electrophoresed, blotted, and probed with SC954 at 1:200.

RESULTS

Cdc2 is expressed in apoptotic profiles in SNpc following either axotomy (Fig. 1A) or intrastriatal 6-OHDA lesion (Fig. 1C). In the two models, cdc2 expression was observed only in rounded apoptotic profiles lacking neuronal cytoplasmic morphology, and which usually contained characteristic, distinct, round, basophilic apoptotic chromatin clumps. All apoptotic profiles that retained neuronal morphology (Fig. 1D) or cytoplasm (Fig. 1E) were cdc2 negative. A small number of cdc2-positive profiles in the axotomy model contained either very faint, small basophilic apoptotic chromatin clumps or none (Fig. 1B). These cdc2-positive profiles which lack clear nuclear chromatin clumps are likely to be apoptotic bodies; we have previously observed similar, small, fragmented profiles with immunohistochemical staining of cdk5 (34). These cdc2-positive apoptotic bodies were present in the axotomy but not in the 6-OHDA model. This difference may be due to the fact that although the induction of PCD following axotomy and 6-OHDA was similar in the total number of apoptotic profiles, the number of cdc2-positive apoptotic profiles in axotomy was approximately three-fold higher than 6-OHDA model (Fig. 2). Since the cdc2-positive apoptotic bodies make up only a small percentage of positive profiles, they may be quite rare in the 6-OHDA model.

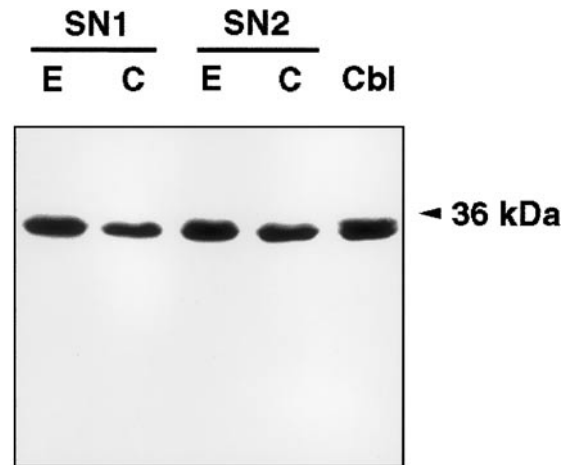


FIG. 3. Western analysis of cdc2 expression in the 6OHDA model. PND7 rats ($n = 4$) underwent intrastriatal injection of 6OHDA and were sacrificed at PLD6. PND2 cerebellar tissue (Cb1) was included as a positive control. Protein concentration of each lysate was determined and 90 μg was loaded per lane. A single band at the expected molecular weight (17) was detected in all lanes. In two representative animals the density of the band is greater in the Experimental (E) SN as compared to the contralateral Control (C). Similar results were obtained in all animals.

TABLE 1

Cellular Phenotypes of Apoptotic Profiles
in the 6OHDA Model

	NeuN	GFAP	OX-42	TOTAL
Sections (n)	13	11	15	39
Apoptotic profiles (n)	133	79	137	349
Apoptotic profiles positive for antigen (%)	20 (15%)	1 (1.3%)	1 (0.7%)	22

Note. Five rats were lesioned with 6-OHDA and consecutive sections were processed for NeuN, GFAP, and OX-42 immunostaining. All Paxinos-Watson plane 4.2 sections were analyzed for the presence of apoptotic profiles identified by thionin-positive chromatin clumps, and the presence of apoptotic profiles immunostained for each antigen. For each antigen, the number of sections, the total number of apoptotic profiles in the sections, and the number (and percentage) of immunostained apoptotic profiles are shown.

The observation of *cdc2* positivity in apoptotic profiles which lack cytoplasmic features is similar to what we have previously found for *cdk5* (34) and it raises a question of what cellular phenotypes give rise to these *cdc2*-positive profiles. For *cdk5*, although all the profiles lacked cytoplasm, we were able to demonstrate that some were neuronal in origin, because *cdk5* immunoreactivity colocalized with NeuN, a neuronal nuclear marker (33, 34, 52). In our previous assessment of *cdk5*, however, we noted that NeuN was often barely detectable, suggesting that as neurons die, they lose expression of this marker, as they do other cellular markers (8). In this study, we were unable to achieve double-labeling for *cdc2* and NeuN. This result has two main interpretations: either *cdc2* is expressed in neurons after they have lost phenotype expression, or it is expressed in nonneuronal cells undergoing apoptosis. To distinguish between these possibilities, we sought to determine the relative numbers of neurons, astrocytes and microglia giving rise to apoptotic profiles in the SNpc in the 6OHDA model. Rats ($n = 5$) were lesioned with 6OHDA and processed for immunohistochemistry for NeuN, GFAP, and OX-42, followed by thionin counterstain. A total of 349 thionin-stained apoptotic profiles were identified among all available Paxinos-Watson 4.2 plane sections from these animals (Table 1). It can be seen that the majority of apoptotic profiles identified by thionin-stained chromatin clumps are not immunostained, and cannot be assigned to any of the three cellular phenotypes, presumably due to loss of cellular markers during the apoptotic process, which has been well-documented for neurons (8). Among those that were immunostained, the large majority (20/22; 91%) were NeuN positive. We conclude that, at a population level, the large majority of apoptotic profiles in this model are likely to derive from neurons, and the *cdc2*-positive profiles are therefore likely to be neuronal in origin.

To ensure monospecificity of the *cdc2* antibody in SN tissue, and to confirm increased expression of *cdc2* in SN following unilateral 6OHDA lesion, Western analysis was performed (Fig. 3). This analysis indicated a single prominent band at the expected molecular weight, confirming the specificity of the antibody. Western analysis also confirmed increased protein expression in the SN upon induction of apoptotic cell death.

A small number of *cdc2*-positive apoptotic profiles with identical cellular morphology (data not shown) were observed on the contralateral control side in the SNpc in both models, where there is no induction of death. These *cdc2*-positive profiles are likely to be due to ongoing natural cell death during this developmental period (22). *Cdc2*-positive staining was also present in a small number of apoptotic profiles due to natural cell death on both sides of the brain in the subthalamic nucleus, cortex, ventral tegmental area, and in cerebellar granule cells (data not shown).

We explored the possible functional significance of this *cdc2* staining by examining the expression of one of the phosphoepitopes it can produce, MPM2 (50). While positive MPM2 immunoperoxidase staining was present in mitotic spindles of cells of unknown phenotype undergoing mitosis in the SN in both models (Fig. 4), there was not a single instance of an apoptotic profile with MPM2 labeling in the SNpc in over 200 profiles in 4 animals in each model. Although *cdc2* is generally expressed in the context of cell cycle regulation, it is possible that cells undergoing apoptosis in the SNpc disintegrate and are eliminated in the G2 phase before entering the M phase and expressing MPM2. Alternatively, errant expression of *cdc2* may not be direct evidence that a neuron has entered a formal cell cycle process. Therefore, to further interpret *cdc2* expression, we examined another cell cycle marker, that of BrdU incorporation. BrdU is an exogenous DNA precursor that is incorporated into DNA strands undergoing replication or repair.

For BrdU incorporation, rats at PLD 1 in the axotomy model and at PLD 6 in the 6-OHDA model (the times of peak induction of cell death) received two intraperitoneal injections of BrdU (50 mg/kg) (Sigma, Saint-Louis, MO) followed by one similar injection the next day 4 h before sacrifice. We have previously shown that normal SN neurons do not incorporate BrdU between PND 3 and PND 12 (7). Immunofluorescence double labeling demonstrated that TH-positive neurons undergoing apoptosis in the SNpc, as demonstrated by Hoechst counterstaining of chromatin clumps, have incorporated BrdU. The colabeling of TH and BrdU in apoptotic profiles in SNpc was present in both axotomy (Fig. 5) and 6-OHDA lesion (Fig. 6) models.

DISCUSSION

We report herein for the first time *in vivo* evidence that postmitotic, postmigratory, differentiated neurons of the SNpc express cell cycle markers before they die by apoptosis. We have demonstrated in two models of postnatal induced PCD, MFB axotomy, and intrastriatal 6-OHDA lesion, that cell cycle markers for the G2 phase (*cdc2*) and the S phase (BrdU incorporation) are expressed. The M-phase marker MPM2 is not. The ectopic expression of *cdc2* was observed not only in induced PCD of neurons of the SNpc but also in apoptotic profiles due to natural cell death in other brain regions. This is the first *in vivo* demonstration that *cdc2* expression may be a general feature of neuronal apoptosis in brain. The *cdc2* kinase controls cell entry into mitosis and initiates the dissolution of the nuclear membrane and promotes chromatin condensation, events that are shared between mitosis and apoptosis (18, 45). It is possible that aberrant *cdc2* activation is a general mechanism for the induction of apoptosis through the initiation of uncoordinated entry into mitosis or, alternatively, its expression may be related to some function unrelated to its role in cell cycle regulation.

Interestingly, the morphologic features we have observed for *cdc2* expression in apoptotic profiles and apoptotic bodies in these two models were quite similar to what we have described for *cdk5* expression in the two models (34). *Cdk5* expression was identified in small, rounded apoptotic profiles which contained chromatin clumps and in adjacent apoptotic bodies which lacked them. The *cdk5* profiles, like *cdc2* profiles, consistently lacked surrounding cytoplasm, and thus appeared to be in a late stage of apoptosis. The appearance of *cdc2* and *cdk5* in morphologically similar apoptotic profiles suggests that these two homologous proteins may be playing a similar role.

Although the morphologic appearance of *cdc2* expression was similar in the axotomy and 6-OHDA models, there were quantitative differences. In the axotomy model, about 30% of apoptotic profiles were *cdc2* positive, whereas in the 6-OHDA model, it was only about 10%. This difference suggests that there may be differences in the mechanisms of cell death operative in the two models. There is a precedent for such, because we have previously found evidence for a difference between the 6-OHDA model and a model of PCD in SN dopamine neurons induced by developmental striatal target injury (29). The 6-OHDA model is less dependent on developmental age, and it shows different patterns of cellular distribution of activated caspase-3 (23) and caspase cleavage products (38). Whether similar differences exist between the axotomy and the 6-OHDA models, and whether they may relate to the

difference in observed prevalence of *cdc2* profiles will require further investigation.

The expression of any single cell cycle marker is not a direct evidence that a cell has in fact entered or traversed the cell cycle. Therefore, we have also examined incorporation of BrdU, an exogenous DNA precursor which is incorporated into DNA undergoing replication (20), several hours before death. Using immunofluorescence double labeling for BrdU and TH, we have shown that postmitotic dopaminergic neurons in the SNpc undergoing apoptosis after either MFB transection (Fig. 5) or 6-OHDA lesion (Fig. 6), as demonstrated by Hoechst counterstain, have intensely incorporated BrdU. This finding provides evidence that dying neurons of the SNpc are expressing sequential cell cycle events. BrdU incorporation suggests that they have reentered the S phase, and expression of *cdc2* suggests that they proceed to G2. However, the cells do not appear to proceed into mitosis as MPM2 was not expressed in these profiles. The fact that *cdc2*-immunopositive staining appeared only in late apoptotic profiles and in apoptotic remnants (Fig. 1B) supports the notion that these dying neurons may be eliminated before entering the M phase. On the other hand, BrdU immunofluorescence labeling was observed in early as well as in late apoptotic profiles in the SNpc since it colabeled with TH found in the cytoplasm (Figs. 5 and 6). The observation that BrdU was incorporated in apoptotic profiles that maintained neuronal shape and cytoplasm and retained its phenotype suggests that DNA synthesis is an earlier event in the apoptosis process. The protocol for BrdU administration was designed to ensure labeling of late and early apoptotic profiles. Rats at PLD 1 in the axotomy model and at PLD 6 in the 6-OHDA model received two intraperitoneal injections of BrdU (50 mg/kg) followed by one similar injection the next day 4 h before sacrifice.

BrdU incorporation is a well-documented technique for investigating cellular events in development such as proliferation, migration, and differentiation (5, 24, 26, 32). A question could be raised about the contribution of DNA repair to the observed labeling in dying or damaged cells. Although DNA repair may contribute to the observed BrdU labeling in dying SNpc neurons, we interpret this finding as more likely to be due to DNA synthesis. BrdU incorporation has been considered a cell cycle marker for DNA synthesis in postmitotic cells undergoing apoptosis in either the presence (4, 20) or absence (35) of PCNA expression which is required as cofactor for the activity of DNA polymerases in normal S-phase and in DNA repair (35). The contribution of DNA repair to the observed BrdU incorporation into apoptotic cells seems unlikely based on the observation that the major base excision repair enzyme, APE/ref-1, which is responsible for recognizing and re-

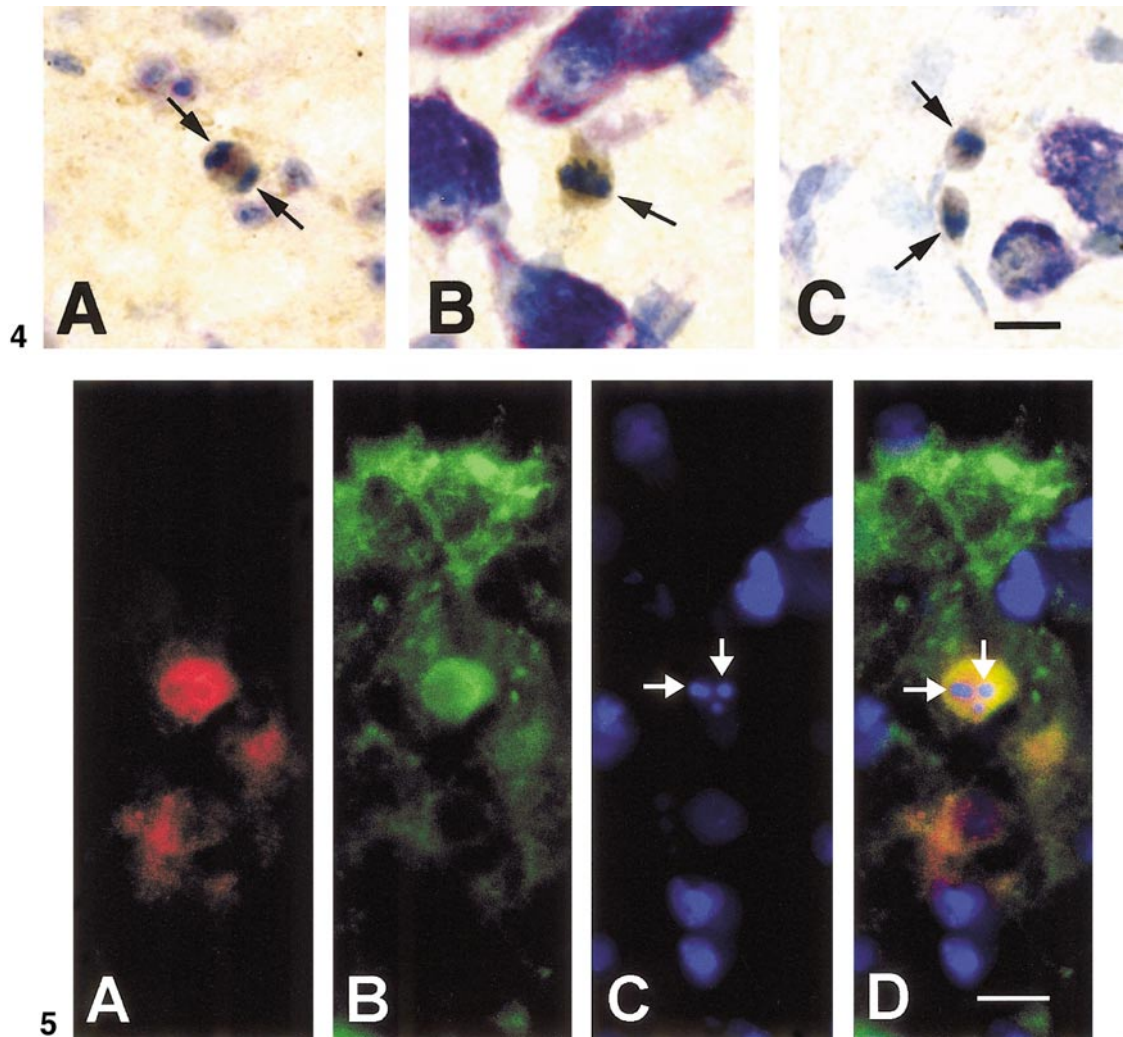


FIG. 4. MPM2 immunoperoxidase stain and thionin counterstain of the SN. Positive staining for MPM2 is observed in SN in profiles at different stages of mitosis. (A) In a PND 9 rat, positive staining for MPM2 is observed in a mitotic profile in late anaphase. Arrows indicate chromosomes stained blue by thionin. (B and C) Positive staining is observed in a PND 13 rat in mitotic figures in metaphase and late telophase, respectively. Bar = 10 μ m.

FIG. 5. Colocalization of BrdU expression with TH in an apoptotic profile in the SNpc on PLD 2 following MFB transection. Panel A shows BrdU (indicated by Texas red) and B shows TH (indicated by green fluorescein). Apoptotic chromatin clumps have been demonstrated in C by counterstain with Hoechst 33342 (blue). Panel D shows a merged image of A, B, and C demonstrating colocalization of BrdU and TH in an apoptotic profile showing round chromatin clumps (arrows). Bar = 10 μ m.

pairing baseless sites in DNA, is dramatically reduced in one model, that of epidermal growth factor-responsive neural progenitor cells undergoing apoptosis (54). This suggests that cells marked for PCD lose one of the key enzymes in DNA base repair. In addition, while DNA degradation is a universal feature of PCD and provides the biochemical basis of TUNEL labeling (13), BrdU incorporation is not. For example, Freeman *et al.* did not observe BrdU labeling in sympathetic neurons deprived of NGF (12). The expression of *cdc2* in vulnerable neurons of Alzheimer's disease is accompanied by aberrant expres-

sion of cell cycle markers of the G1/S phase such as cyclin D1, Cdk4, PCNA, and cyclin B1 (1, 21, 50). Recently, Yang *et al.* (2001) showed direct evidence that the immunocytochemical appearance of cell cycle proteins in dying neurons of Alzheimer's disease is accompanied by a reentry into mitosis. Using fluorescent *in situ* hybridization to examine the chromosomal complement of interphase neuronal nuclei, they demonstrated that hippocampal pyramidal and basal forebrain neurons in Alzheimer's disease have fully or partially replicated four separate loci on three different chromosomes (53). Based on these

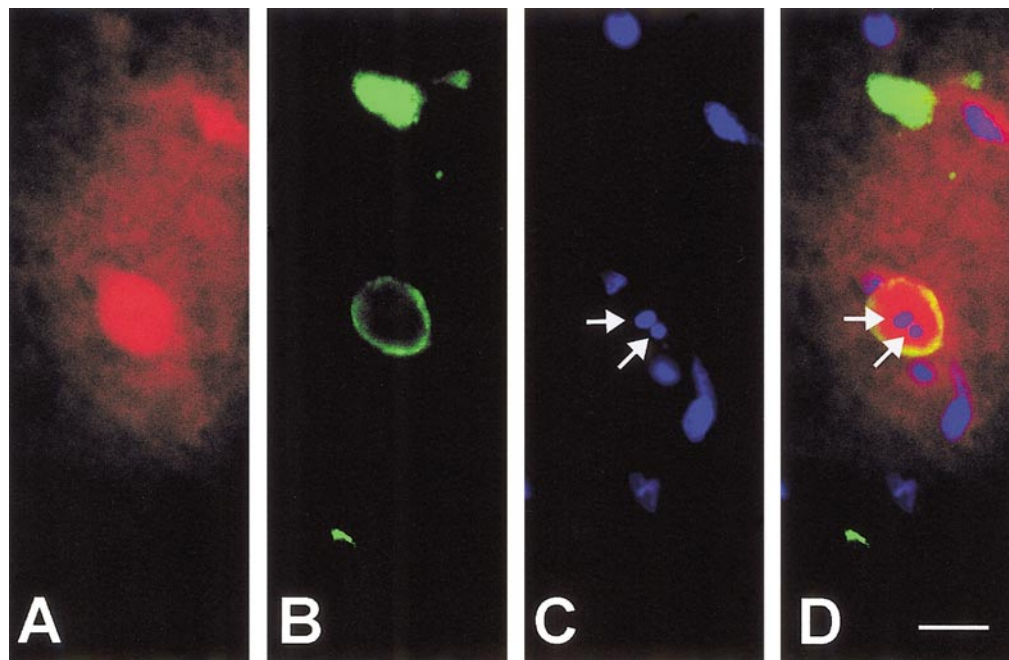


FIG. 6. Colocalization of BrdU expression with TH in an apoptotic profile in the SNpc on PLD 7 following intrastriatal 6-OHDA lesion. Panels A and B show BrdU (indicated by Texas red) and TH (indicated by green fluorescein) immunostaining, respectively. (C) Apoptotic chromatin clumps as demonstrated by Hoechst 33342 (blue). Panel D shows a merged image of A, B, and C that demonstrates colocalization of BrdU and TH in an apoptotic profile. Bar = 10 μ m.

considerations, we believe that BrdU incorporation in dopamine neurons undergoing apoptosis is more likely to reflect DNA synthesis than repair.

This study provides additional support for the emerging hypothesis that apoptosis in postmitotic neurons is a consequence of an aberrant attempt to reenter the cell cycle. It provides *in vivo* evidence that postmitotic neurons of the SNpc undergoing PCD after either neonatal MFB transection or intra-striatal 6-OHDA lesion express markers for S phase and G2 phase and are eliminated before traversing the M phase. Since these are both animal models of induced PCD in the SNpc this study raises the question whether activation of cell cycle regulatory proteins may play a role in the demise of dopaminergic neurons in Parkinson's disease, in which PCD has been postulated to play a role (49).

ACKNOWLEDGMENTS

This work was supported by NS 26836, NS38370, The Parkinson's Disease Foundation, and by the Lowenstein Foundation.

REFERENCES

1. Busser, J., D. S. Geldmacher, and K. Herrup. 1998. Ectopic cell cycle proteins predict the sites of neuronal cell death in Alzheimer's disease brain. *J. Neurosci.* **18**: 2801–2807.
2. Buttyan, R., Z. Zakeri, R. Lockshin, and D. Wolgemuth. 1988. Cascade induction of c-fos, c-myc, and heat shock 70K transcripts during regression of the rat ventral prostate gland. *Mol. Endocrinol.* **2**: 650–657.
3. Clarke, P. G. H., and R. W. Oppenheim. 1995. Neuron death in vertebrate development: *In vivo* methods. In *Methods in Cell Biology: Cell Death* (L. M. Schwartz and B. A. Osborne, Eds.), pp. 277–321. Academic Press, New York.
4. Colombel, M., C. A. Olsson, P.-Y. Ng, and R. Buttyan. 1992. Hormone-regulated apoptosis results from reentry of differentiated prostate cells onto a defective cell cycle. *Cancer Res.* **52**: 4313–4319.
5. Dolbeare, F. 1995. Bromodeoxyuridine: A diagnostic tool in biology and medicine, Part I: Historical perspectives, histochemical methods and cell kinetics. *Histochem. J.* **27**: 339–369.
6. El-Khodori, B. F., and R. E. Burke. 2002. Medial forebrain bundle axotomy during development induces apoptosis in dopamine neurons of the substantia nigra and activation of caspases in their degenerating axons. *J. Comp. Neurol.* **452**: 65–79.
7. El-Khodori, B. F., N. G. Kholodilov, O. Yarygina, and R. E. Burke. 2001. The expression of mRNAs for the proteasome complex is developmentally regulated in the rat mesencephalon. *Brain Res. Dev. Brain Res.* **129**: 47–56.
8. Estus, S., W. J. Zaks, R. S. Freeman, M. Gruda, R. Bravo, and E. M. Johnson. 1994. Altered gene expression in neurons during programmed cell death identification of c-jun as necessary for neuronal apoptosis. *J. Cell Biol.* **127**: 1717–1727.
9. Evan, G. I., A. H. Wyllie, C. S. Gilbert, T. D. Littlewood, H. Land, M. Brooks, C. M. Waters, L. Z. Penn, and D. C. Hancock. 1992. Induction of apoptosis in fibroblasts by c-myc protein. *Cell* **69**: 119–128.

10. Feddersen, R. M., R. Ehlenfeldt, W. S. Yunis, H. B. Clark, and H. T. Orr. 1992. Disrupted cerebellar cortical development and progressive degeneration of Purkinje cells in SV40 T antigen transgenic mice. *Neuron* **9**: 955–966.
11. Ferrari, G. and L. A. Greene. 1994. Proliferative inhibition by dominant-negative Ras rescues naive and neuronally differentiated PC12 cells from apoptotic death. *EMBO J.* **13**: 5922–5928.
12. Freeman, R. S., S. Estus, and E. M. Johnson. 1994. Analysis of cell cycle related gene expression in postmitotic neurons selective induction of cyclin D1 during programmed cell death. *Neuron* **12**: 343–355.
13. Gavrieli, Y., Y. Sherman, and S. A. Ben-Sasson. 1992. Identification of programmed cell death in situ via specific labeling of nuclear DNA fragmentation. *J. Cell Biol.* **119**: 493–501.
14. Giovanni, A., F. Wirtz-Brugger, E. Keramaris, R. Slack, and D. S. Park. 1999. Involvement of cell cycle elements, cyclin-dependent kinases, pRb, and E2F × DP, in B-amyloid-induced neuronal death. *J. Biol. Chem.* **274**: 19011–19016.
15. Gundersen, H. J. G. 1986. Stereology of arbitrary particles. *J. Microsc.* **143**: 3–45.
16. Hammang, J. P., R. R. Behringer, E. E. Baetge, R. D. Palmiter, R. L. Brinster, and A. Messing. 1993. Oncogene expression in retinal horizontal cells of transgenic mice results in a cascade of neurodegeneration. *Neuron* **10**: 1197–1209.
17. Hayes, T. E., N. L. Valtz, and R. D. McKay. 1991. Downregulation of CDC2 upon terminal differentiation of neurons. *New Biol.* **3**: 259–269.
18. Heald, R. and F. McKeon. 1990. Mutations of phosphorylation sites in lamin A that prevent nuclear lamina disassembly in mitosis. *Cell* **61**: 579–589.
19. Heller, A., J. O. Hutchens, M. L. Kirby, F. Karapas, and C. Fernandez. 1979. Stereotaxic electrode placement in the neonatal rat. *J. Neurosci. Methods* **1**: 41–76.
20. Herrup, K. and J. C. Busser. 1995. The induction of multiple cell cycle events precedes target-related neuronal death. *Development* **121**: 2385–2395.
21. Husseman, J. W., D. Nochlin, and I. Vincent. 2000. Mitotic activation: A convergent mechanism for a cohort of neurodegenerative diseases. *Neurobiol. Aging* **21**: 815–828.
22. Janec, E. and R. E. Burke. 1993. Naturally occurring cell death during postnatal development of the substantia nigra of the rat. *Mol. Cell. Neurosci.* **4**: 30–35.
23. Jeon, B. S., N. G. Kholodilov, T. F. Oo, S. Kim, K. J. Tomaselli, A. Srinivasan, L. Stefanis, and R. E. Burke. 1999. Activation of caspase-3 in developmental models of programmed cell death in neurons of the substantia nigra. *J. Neurochem.* **73**: 322–333.
24. Kawano, H., K. Ohyama, K. Kawamura, and I. Nagatsu. 1995. Migration of dopaminergic neurons in the embryonic mesencephalon of mice. *Brain Res. Dev. Brain Res.* **86**: 101–113.
25. Kranenburg, O., A. J. van der Eb, and A. Zantema. 1996. Cyclin D1 is an essential mediator of apoptotic neuronal cell death. *EMBO J.* **15**: 46–54.
26. Kuhn, H. G., H. Dickinson-Anson, and F. H. Gage. 1996. Neurogenesis in the dentate gyrus of the adult rat: Age-related decrease of neuronal progenitor proliferation. *J. Neurosci.* **16**: 2027–2033.
27. Lauder, J. M. and F. E. Bloom. 1974. Ontogeny of monoamine neurons in the locus coeruleus, raphe nuclei and substantia nigra of the rat. *J. Comp. Neurol.* **155**: 469–482.
28. Lundberg, A. S. and R. A. Weinberg. 1999. Control of the cell cycle and apoptosis. *Eur. J. Cancer* **35**: 1886–1894.
29. Macaya, A., F. Munell, R. M. Gubits, and R. E. Burke. 1994. Apoptosis in substantia nigra following developmental striatal excitotoxic injury. *Proc. Natl. Acad. Sci. USA* **91**: 8117–8121.
30. Marchand, R. and L. J. Poirer. 1983. Isthmic origin of neurons of the rat substantia nigra. *Neuroscience* **9**: 373–381.
31. Marti, M. J., C. J. James, T. F. Oo, W. J. Kelly, and R. E. Burke. 1997. Early developmental destruction of terminals in the striatal target induces apoptosis in dopamine neurons of the substantia nigra. *J. Neurosci.* **17**: 2030–2039.
32. Miller, M. W. and R. S. Nowakowski. 1988. Use of bromodeoxyuridine-immunohistochemistry to examine the proliferation, migration and time of origin of cells in the central nervous system. *Brain Res.* **457**: 44–52.
33. Mullen, R. J., C. R. Buck, and A. M. Smith. 1992. NeuN, a neuronal specific nuclear protein in vertebrates. *Development* **116**: 201–211.
34. Neystat, M., M. Rzhetskaya, T. F. Oo, N. Kholodilov, O. Yarygina, A. Wilson, B. F. El-Khodori, and R. E. Burke. 2001. Expression of cyclin-dependent kinase 5 and its activator p35 in models of induced apoptotic death in neurons of the substantia nigra in vivo. *J. Neurochem.* **77**: 1611–1625.
35. Ninomiya, Y., R. Adams, G. M. Morriss-Kay, and K. Eto. 1997. Apoptotic cell death in neuronal differentiation of P19 EC cells: Cell death follows reentry into S phase. *J. Cell. Physiol.* **172**: 25–35.
36. O'Connor, L., D. C. Huang, L. A. O'Reilly, and A. Strasser. 2000. Apoptosis and cell division. *Curr. Opin. Cell Biol.* **12**: 257–263.
37. Oo, T. F. and R. E. Burke. 1997. The time course of developmental cell death in phenotypically defined dopaminergic neurons of the substantia nigra. *Dev. Brain Res.* **98**: 191–196.
38. Oo, T. F., R. Siman, and R. E. Burke. 2002. Distinct nuclear and cytoplasmic localization of caspase cleavage products in two models of induced apoptotic death in dopamine neurons of the substantia nigra. *Exp. Neurol.* **175**: 1–9.
39. Park, D. S., S. E. Farinelli, and L. A. Greene. 1996. Inhibitors of cyclin-dependent kinases promote survival of post-mitotic neuronally differentiated PC12 cells and sympathetic neurons. *J. Biol. Chem.* **271**: 8161–8169.
40. Park, D. S., B. Levine, G. Ferrari, and L. A. Greene. 1997. Cyclin dependent kinase inhibitors and dominant negative cyclin dependent kinase 4 and 6 promote survival of NGF-deprived sympathetic neurons. *J. Neurosci.* **17**: 8975–8983.
41. Park, D. S., E. J. Morris, R. Bremner, E. Keramaris, J. Padmanabhan, M. Rosenbaum, M. L. Shelanski, H. M. Geller, and L. A. Greene. 2000. Involvement of retinoblastoma family members and E2F/DP complexes in the death of neurons evoked by DNA damage. *J. Neurosci.* **20**: 3104–3114.
42. Park, D. S., E. J. Morris, L. A. Greene, and H. M. Geller. 1997. G1/S cell cycle blockers and inhibitors of cyclin-dependent kinases suppress camptothecin-induced neuronal apoptosis. *J. Neurosci.* **17**: 1256–1270.
43. Park, D. S., E. J. Morris, J. Padmanabhan, M. L. Shelanski, H. M. Geller, and L. A. Greene. 1998. Cyclin-dependent kinases participate in death of neurons evoked by DNA-damaging agents. *J. Cell Biol.* **143**: 457–467.
44. Paxinos, G. and C. Watson. 1982. *The Rat Brain in Stereotaxic Coordinates*. Academic Press, San Diego.
45. Shi, L., W. K. Nishioka, J. Th'ng, E. M. Bradbury, D. W. Litchfield, and A. H. Greenberg. 1994. Premature p34^{cdc2} activation required for apoptosis. *Science* **263**: 1143–1145.
46. Shi, Y., J. M. Glynn, L. J. Guilbert, T. G. Cotter, R. P. Bissonnette, and D. R. Green. 1992. Role for c-myc in activation-induced apoptotic cell death in T cell hybridomas. *Science* **257**: 212–214.

47. Shults, C. W., R. Hasimoto, R. M. Brady, and F. H. Gage. 1990. Dopaminergic cells align along radial glia in the developing mesencephalon of the rat. *Neuroscience* **38**: 427–436.
48. Thomaïdou, D., M. C. Mione, J. F. Cavanagh, and J. G. Parnavelas. 1997. Apoptosis and its relation to the cell cycle in the developing cerebral cortex. *J. Neurosci.* **17**: 1075–1085.
49. Tompkins, M. M., E. J. Basgall, E. Zamrini, and W. D. Hill. 1997. Apoptotic-like changes in Lewy-body-associated disorders and normal aging in substantia nigral neurons. *Am. J. Pathol.* **150**: 119–131.
50. Vincent, I., G. Jicha, M. Rosado, and D. W. Dickson. 1997. Aberrant expression of mitotic cdc2/cyclin B1 kinase in degenerating neurons of Alzheimer's disease brain. *J. Neurosci.* **17**: 3588–3598.
51. Vincent, I., M. Rosado, and P. Davies. 1996. Mitotic mechanisms in Alzheimer's disease? *J. Cell Biol.* **132**: 413–425.
52. Wolf, H. K., R. Buslei, R. Schmidt-Kastner, P. K. Schmidt-Kastner, T. Pietsch, O. D. Wiestler, and I. Blumcke. 1996. NeuN: A useful neuronal marker for diagnostic histopathology. *J. Histochem. Cytochem.* **44**: 1167–1171.
53. Yang, Y., D. S. Geldmacher, and K. Herrup. 2001. DNA replication precedes neuronal cell death in Alzheimer's disease. *J. Neurosci.* **21**: 2661–2668.
54. Zhou, F. C., M. R. Kelley, Y. H. Chiang, and P. Young. 2000. Three to four-year-old nonpassaged EGF-responsive neural progenitor cells: Proliferation, apoptosis, and DNA repair. *Exp. Neurol.* **164**: 200–208.